NASA/TM-2012-216310

Dual-Doppler Feasibility Study

Lisa L. Huddleston
Applied Meteorology Unit
Kennedy Space Center, Florida

April 2012

NASA STI Program ... in Profile

Since its founding, NASA has been dedicated to the advancement of aeronautics and space science. The NASA scientific and technical information (STI) program plays a key part in helping NASA maintain this important role.

The NASA STI program operates under the auspices of the Agency Chief Information Officer. It collects, organizes, provides for archiving, and disseminates NASA's STI. The NASA STI program provides access to the NASA Aeronautics and Space Database and its public interface, the NASA Technical Report Server, thus providing one of the largest collections of aeronautical and space science STI in the world. Results are published in both non-NASA channels and by NASA in the NASA STI Report Series, which includes the following report types:

- TECHNICAL PUBLICATION. Reports of completed research or a major significant phase of research that present the results of NASA Programs and include extensive data or theoretical analysis. Includes compilations of significant scientific and technical data and information deemed to be of continuing reference value. NASA counter-part of peer-reviewed formal professional papers but has less stringent limitations on manuscript length and extent of graphic presentations.

- TECHNICAL MEMORANDUM. Scientific and technical findings that are preliminary or of specialized interest, e.g., quick release reports, working papers, and bibliographies that contain minimal annotation. Does not contain extensive analysis.

- CONTRACTOR REPORT. Scientific and technical findings by NASA-sponsored contractors and grantees.

- CONFERENCE PUBLICATION. Collected papers from scientific and technical conferences, symposia, seminars, or other meetings sponsored or co-sponsored by NASA.

- SPECIAL PUBLICATION. Scientific, technical, or historical information from NASA programs, projects, and missions, often concerned with subjects having substantial public interest.

- TECHNICAL TRANSLATION. English-language translations of foreign scientific and technical material pertinent to NASA's mission.

Specialized services also include organizing and publishing research results, distributing specialized research announcements and feeds, providing help desk and personal search support, and enabling data exchange services.

For more information about the NASA STI program, see the following:

- Access the NASA STI program home page at *http://www.sti.nasa.gov*

- E-mail your question via the Internet to help@sti.nasa.gov

- Fax your question to the NASA STI Help Desk at 443-757-5803

- Phone the NASA STI Help Desk at 443-757-5802

- Write to:
  NASA STI Help Desk
  NASA Center for AeroSpace Information
  7115 Standard Drive
  Hanover, MD 21076-1320

NASA/TM-2012-216310

Dual-Doppler Feasibility Study

Lisa L. Huddleston
Applied Meteorology Unit
Kennedy Space Center, Florida

National Aeronautics and
Space Administration

Kennedy Space Center
Kennedy Space Center, FL 32899-0001

April 2012

Acknowledgements

The author thanks Mr. William Roeder, Mr. Todd McNamara, and Mr. Jon Saul of the 45th Weather Squadron for their technical guidance on this project. In addition, thanks go to Mr. Dave Sharp and Mr. Matt Volkmer of the National Weather Service in Melbourne, Fla. for their assistance in understanding the NOAA products available for dual-Doppler analysis and in obtaining the specifications for the WSR-88D radar. Finally, the author would like to thank Ms. Winnie Crawford of the Applied Meteorology Unit and Dr. Frank Merceret of the KSC Weather Office for their participation in extensive discussions of the subject matter included in this report and for their editorial expertise.

Available from:

NASA Center for AeroSpace Information
7121 Standard Drive
Hanover, MD 21076-1320
(301) 621-0390

This report is also available in electronic form at

http://science.ksc.nasa.gov/amu/

Executive Summary

When two or more Doppler weather radar systems are monitoring the same region, the Doppler velocities can be combined to form a three-dimensional (3-D) wind vector field thus providing for a more intuitive analysis of the wind field. A real-time display of the 3-D winds can assist forecasters in predicting the onset of convection and severe weather. The data can also be used to initialize local numerical weather prediction models. Two operational Doppler Radar systems are in the vicinity of Kennedy Space Center (KSC) and Cape Canaveral Air Force Station (CCAFS); these systems are operated by the 45th Space Wing (45 SW) and the National Weather Service Melbourne, Fla. (NWS MLB). Dual-Doppler applications were considered by the 45 SW in choosing the site for the new radar. Accordingly, the 45th Weather Squadron (45 WS), NWS MLB and the National Aeronautics and Space Administration tasked the Applied Meteorology Unit (AMU) to investigate the feasibility of establishing dual-Doppler capability using the two existing systems. This study investigated technical, hardware, and software requirements necessary to enable the establishment of a dual-Doppler capability.

Review of the available literature pertaining to the dual-Doppler technique and consultation with experts revealed that the physical locations and resulting beam crossing angles of the 45 SW and NWS MLB radars make them ideally suited for a dual-Doppler capability. The dual-Doppler equations were derived to facilitate complete understanding of dual-Doppler synthesis; to determine the technical information requirements; and to determine the components of wind velocity from the equation of continuity and radial velocity data collected by the two Doppler radars. Analysis confirmed the suitability of the existing systems to provide the desired capability. In addition, it is possible that both 45 SW radar data and Terminal Doppler Weather Radar data from Orlando International Airport could be used to alleviate any radar geometry issues at the NWS MLB radar, such as the "cone of silence" or beam blockage. In the event of a radar outage at one of the sites, the multi-radar algorithms would provide continuing coverage of the area through use of the data from the remaining operational radar sites.

There are several options to collect, edit, synthesize and display dual-Doppler data sets. These options include commercial packages available for purchase and a variety of freeware packages available from the National Center for Atmospheric Research (NCAR) for processing raw radar data. However, evaluation of the freeware packages revealed that they do not have sufficient documentation and configuration control to be certified for 45 SW use. Additionally, a T1 data line must be installed/leased from the NWS MLB office and CCAFS to enable the receipt of NWS MLB raw radar data to use in the dual-Doppler synthesis. Integration of the T1 data line into the Eastern Range infrastructure that will meet the security requirements necessary for 45 SW use is time-consuming and costly.

Overall evaluation indicates that establishment of the dual-Doppler capability using the existing operational radar systems is desirable and feasible with no technical concerns. Installation of such a system represents a significant enhancement to forecasting capabilities at the 45 WS and at NWS MLB. However, data security and cost considerations must be evaluated in light of current budgetary constraints. In any case, gaining the dual-Doppler capability will provide opportunities for better visualization of the wind field and better forecasting of the onset of convection and severe weather events to support space launch operations at KSC and CCAFS.

Table of Contents

List of Figures

List of Tables

1. Introduction

When two or more Doppler weather radar systems are monitoring the same region, the Doppler velocities can be combined to form a three-dimensional (3-D) wind vector field. Such a wind field allows a more intuitive analysis of the 3-D winds, especially for users with little or no experience in deciphering Doppler velocities (Bousquet 2004). A real-time display of the wind field can assist forecasters in predicting the onset of convection and severe weather. The data can also be used to initialize local numerical weather models. Two Doppler radars are in the vicinity of Kennedy Space Center (KSC) and Cape Canaveral Air Force Station (CCAFS): the 45th Space Wing (45 SW) RadTec 43/250 radar and the National Weather Service (NWS) office in Melbourne, Fla. (MLB) Weather Surveillance Radar - 1988 Doppler (WSR-88D) radar. The orientation of these radars with KSC and CCAFS are shown in Figure 1. The 45th Weather Squadron (45 WS), NWS MLB and National Aeronautics and Space Administration (NASA) customers tasked the Applied Meteorology Unit (AMU) to investigate the feasibility of establishing dual-Doppler capability using these two systems. This task summarizes a literature review and consultation with experts to determine technical, hardware, and software requirements necessary to create a dual-Doppler capability. The AMU also investigated cost considerations and viable alternatives.

Developing a dual-Doppler capability can provide a real-time horizontal wind field display to assist 45 WS and NWS forecasters in predicting the onset of convection and severe weather events. These data can also be used to initialize a local mesoscale numerical weather prediction model. In addition, data combined from two or more radars mitigate radar geometry problems such as the cone of silence and beam blockage. (Lakshmanan et al. 2007)

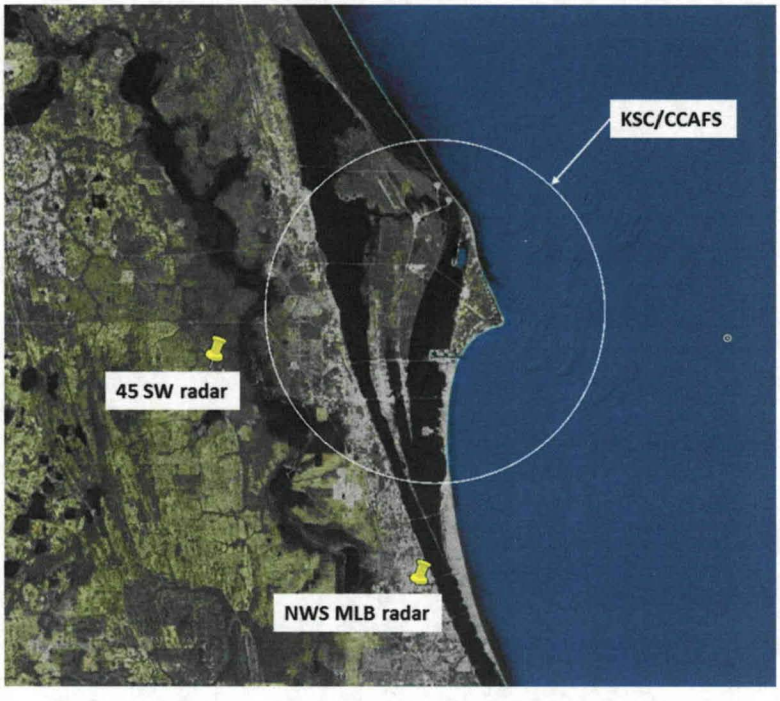

Figure 1. Orientation of the 45 SW radar and the NWS MLB radars with respect to KSC and CCAFS.

2. Principles of Dual-Doppler Radar Measurements

With traditional single Doppler radar, only the radial component of the wind field can be measured. When two or more Doppler radars are surveying an area, the Doppler velocities can be combined to estimate the 3-D wind field. Each individual radar system scans according to its own particular strategy and time, therefore the velocities from each radar must be merged to a common coordinate system and reference time before wind synthesis can occur (Friedrich and Hagen 2004).

The main objective of multiple-Doppler analyses, which combine observations collected by several neighboring Doppler radars to construct the 3-D wind field, is to ease the interpretation of airflow and to provide detailed information on the kinematics of observed storms that even a non-radar specialist can easily understand. Knowledge of storm kinematic structure can provide interesting insights on the storm dynamics through revealing mesoscale wind features that would be difficult to ascertain from just the radial velocity field. Another unique benefit of dual- or multiple-Doppler wind synthesis is to provide information on the structure of the vertical motion field (Bousquet, et al. 2008).

2.1 Dual-Doppler Equation Derivations

The AMU derived the dual-Doppler equations to facilitate complete understanding of dual-Doppler synthesis, to determine the technical information requirements, and to determine how to find the three components of wind velocity from the continuity equation and radial velocity data from two Doppler radars (Armijo 1969). The derivations are available in the Appendix of this report for the interested reader. The dual-Doppler equations were compiled from a combination of the methods of Armijo (1969), Obrien (1970), Lhermitte and Miller (1970) and Carey (2005). The geometry of the radial distance between two radars and a point in space is shown in Figure 2. The typical beam geometry for a single radar is shown in Figure 3.

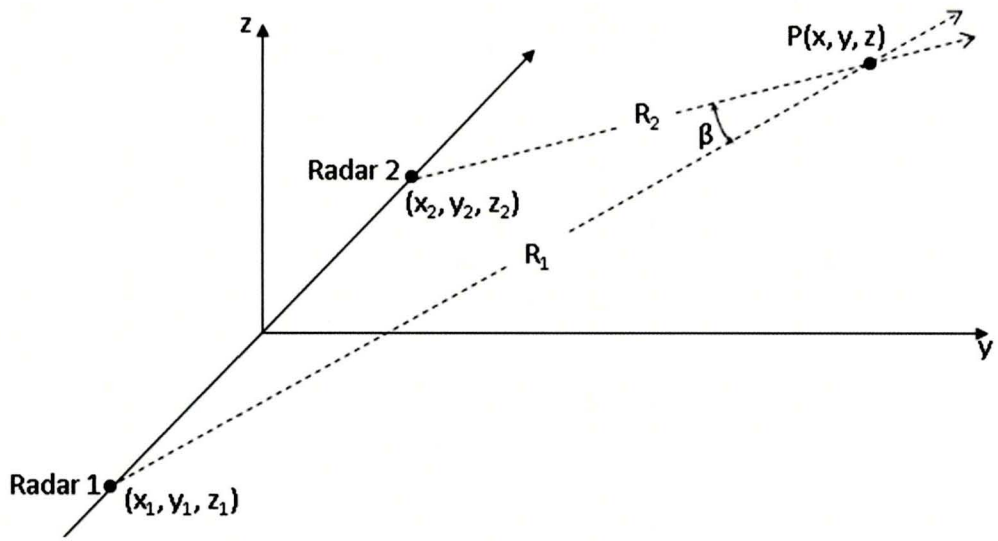

Figure 2. The geometry of the radial distance (R) between radars and a point in space. The target point of the radars is at P(x, y, z). Radar 1 is at point (x_1, y_1, z_1) and radar 2 is at point (x_2, y_2, z_2). Adapted from Figure 9.3 in Doviak and Zrnic (1993).

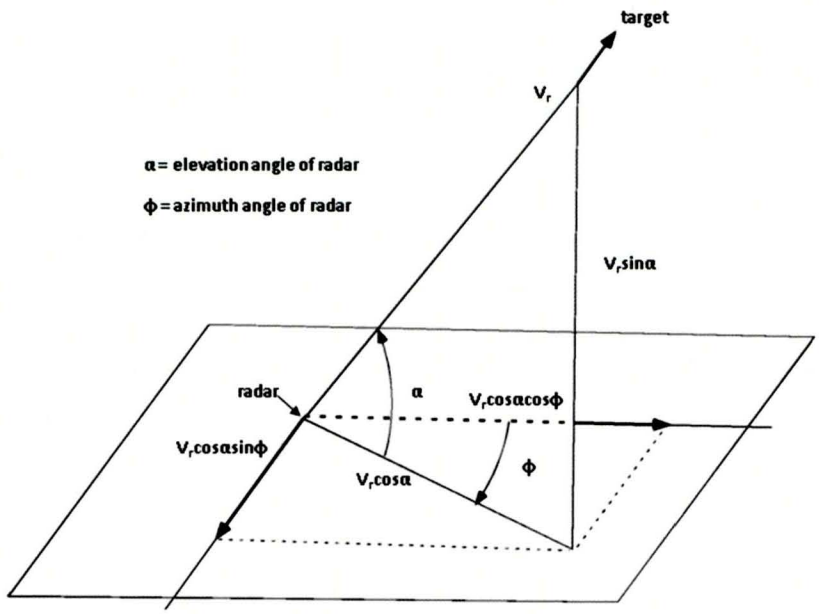

Figure 3. The typical beam geometry for a single radar. Adapted from Figure 6.2 in Rinehart (2004).

2.2 Dual-Doppler Area Geometry

When planning a dual-Doppler capability, the specific area of interest must be studied to determine if the locations of the radars will allow an accurate wind field calculation. Dual-Doppler coverage depends on

- The minimum spatial resolution needed to resolve the weather phenomena of interest,
- The largest acceptable error in horizontal velocity, and
- The distance between the radars (Davies-Jones 1979).
- The orientation of the radars relative to the area for which dual-Doppler coverage is desired.

2.2.1 Optimal vs. Actual Arrangement of Radars

To begin the analysis, unit vectors of the two radial velocities intersect an angle, β (Davies-Jones 1979, Friedrich and Hagen 2004). Using the schematic in Figure 2 as an example, β is the angle between R_1 and R_2 at P. The error variances, σ_u^2 and σ_v^2, of u- and v- wind components are related to the Doppler mean velocity error variances of the two individual radars, σ_1^2 and σ_2^2, by (Davies-Jones 1979):

$$\frac{\sigma_u^2 + \sigma_v^2}{\sigma_1^2 + \sigma_2^2} = \csc^2 \beta.$$

The optimal β that will provide the most accurate wind synthesis is 90° (Beck 2004). Experience at the National Severe Storms Laboratory (NSSL) has shown that a β of ≥ 30° and ≤ 150° is adequate for accurate wind synthesis (Davies-Jones 1979). Outside of this range, a large component of both beams is oriented in the same direction. This will cause large errors in the velocity components derived from the dual-Doppler wind synthesis. The calculated beam crossing angle between the 45 SW and the NWS MLB radars for launch complexes 17A (Figure 4a) and 41 (Figure 4b) on CCAFS are 67.9° and 52.2°, respectively, both within the 30° to 150° range recommended by Davies-Jones (1979).

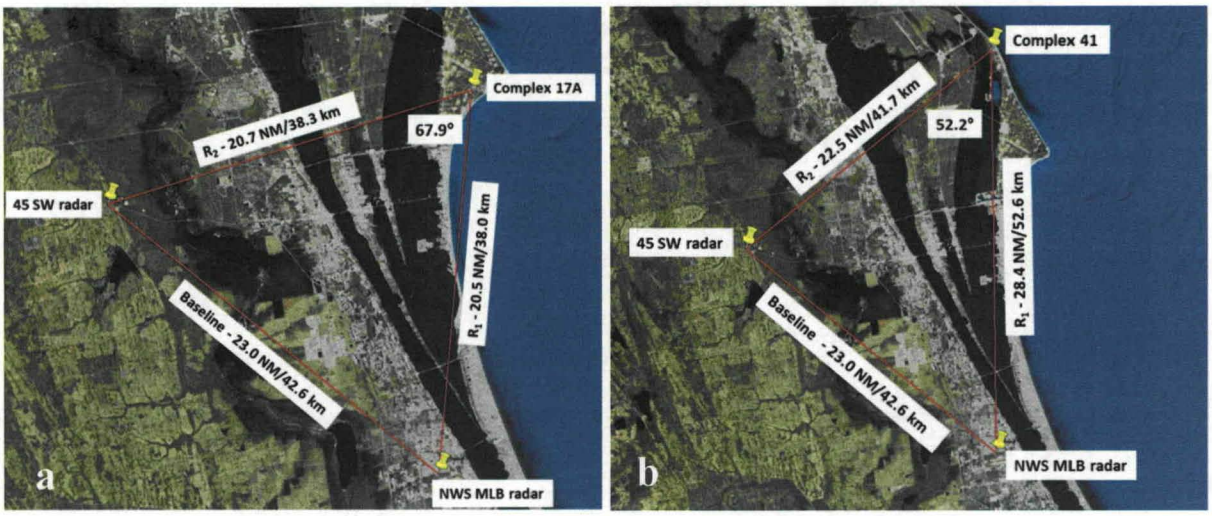

Figure 4. a) The beam crossing angle between the 45 SW and NWS MLB radars for launch complexes 17A (67.9°) and b) 41 (52.2°) on CCAFS. The yellow pins show the locations of the radars. The red lines labeled R_1 and R_2 are analogous to the similarly labeled lines in Figure 2.

The spatial resolution of the dual-Doppler coverage area is related to the baseline, or horizontal distance between two radars. Davies-Jones (1979) and Friedrich and Hagen (2004) proposed that the optimal distance between two radars would range between 23.2 NM (43 km) and 43.7 NM (81 km). Examination of Figure 3 shows that the baseline between the 45 SW and NWS MLB radars is 23 NM (42.6 km), at the low end of the optimal separation distance. The beam crossing angles over KSC and CCAFS and the baseline of the 45 SW and NWS MLB radars makes them ideally suited for a dual-Doppler capability. A critical element of site location is the technical trade-off between velocity component accuracy and spatial resolution (Davies-Jones, 1979). This placement was considered by the 45 WS during the original 45 SW radar site location determination.

2.2.2 Dual-Doppler Area for 45 SW and NWS-MLB Radars

The next step in the analysis is to calculate the total coverage area of the dual-Doppler analysis. Davies-Jones (1979) and Friedrich and Hagen (2004) show that the total coverage area is the intersection of the area (A_1) defined by the upper limits on velocity error variance (Figure 5a) and the area (A_2) defined by the maximum range of the radars (Figure 5b). The area A_1 is made up of two circular areas called dual-Doppler lobes. In the formula for A_1 (Davies-Jones 1979) shown in Figure 5a, d is half of the baseline (23 NM/2 = 11.5 NM) and β is the minimum beam crossing angle in radians ($\pi/6$ rad or 30°). In the formula for A_2 in Figure 5b, R is the maximum range from any point in area A_1 to either of the radars. R for the 45 SW and NWS MLB radar pair is given by (Davies-Jones 1979)

$$2*d*\csc\beta = 2*(11.51 \text{ NM})*\csc(30^\circ) = 46.1 \text{ NM } (85.3 \text{ km}).$$

Area A_2 is the maximum area that can be covered by two radars at an elevation angle of 0°. With increasing elevation, area A_2 decreases (Friedrich and Hagen 2004, Davies-Jones 1979). The dual-Doppler coverage area is defined as the area common to both A_1 and A_2 (Davies-Jones 1979):

$$A_{12}(\beta, R) = A_1(\beta) \cap A_2(R)$$

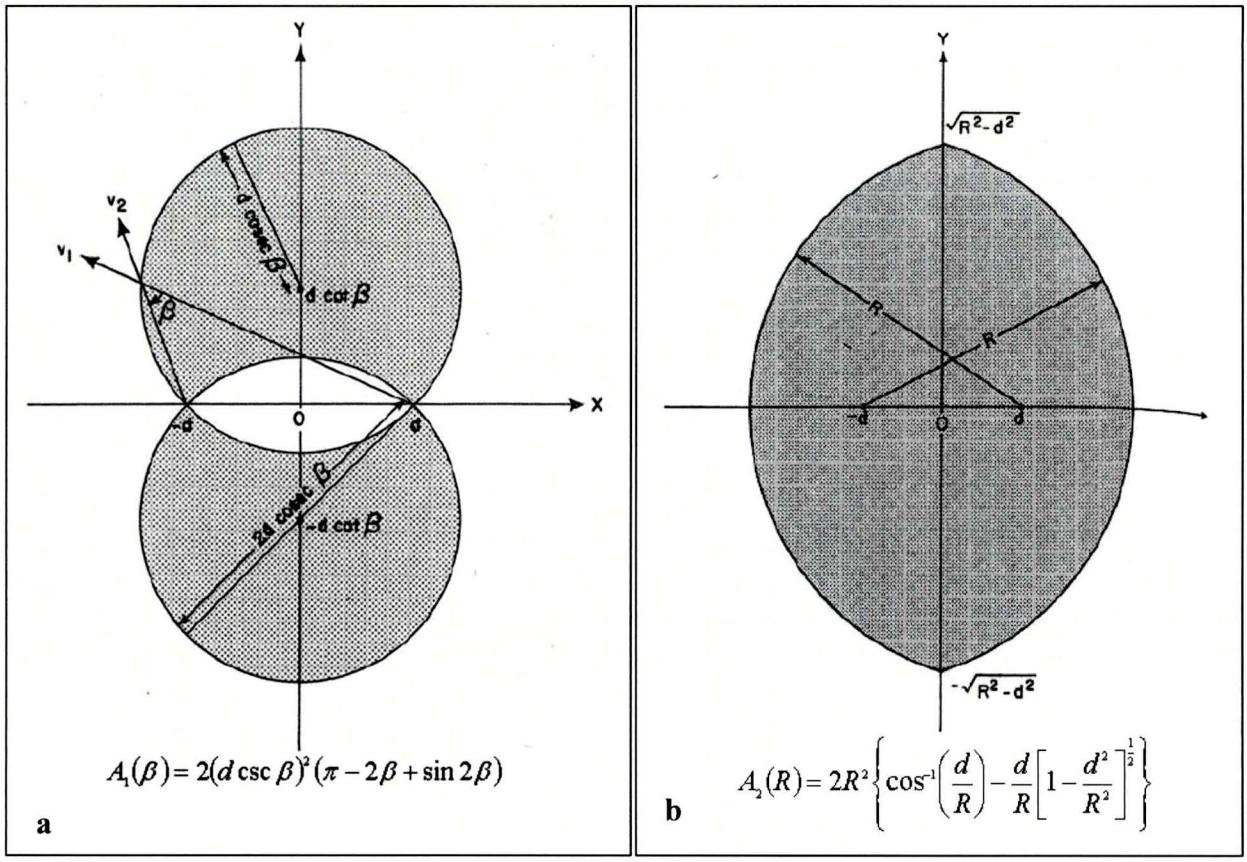

Figure 5. a) Area A_1 that shows the dual-Doppler lobes as stippled areas bounded by $\beta = 30°$ ($\pi/6$ rad) (Figure 1a in Davies-Jones 1979), and b) Area A_2, shown as a stippled area that lies within distance R of both radars (Figure 1b in Davies-Jones 1979).

In a dual-Doppler analysis, the resolution of the resulting merged data is defined as $s = R\pi\Delta/180$, where Δ is the half power beam width in degrees of the radars (Davies-Jones 1979). The technical specifications for the NWS MLB WSR-88D and the 45 SW Radtec 43/250 radars are shown in Table 1. Using these values, the resolution of the 45 SW and NWS MLB radar pair is

$$s = (46.1 \text{ NM})*\pi*(0.95^\circ)/180 = 0.76 \text{ NM } (1.41 \text{ km}).$$

Using the formula for A_1 shown in Figure 5a, the coverage area A_1 of the radar pair is 3,140.2 NM^2 (10,770.7 km^2). Area A_1 for the 45 SW and NWS MLB radars is shown in Figure 6a. The maximum area that can be covered by the radar pair at an elevation angle of 0° is calculated using the formula for area A_2 shown in Figure 5b. This area is shown in Figure 6b and is 4,565.6 NM^2 (15,659.7 km^2). The size of area A_1 fits into the size of area A_2 and is shown in Figure 7. Therefore the area common to both A_1 and A_2 for the 45 SW and NWS MLB radar pair is 3,140.2 NM^2 (10,770.7 km^2). However, the maximum area that can be covered by a radar pair decreases with increasing elevation angle (Davies-Jones 1979, Friedrich and Hagen 2004).

Table 1. Technical specifications for the NWS MLB WSR-88D and 45 SW Radtec 43/250 radars.

Parameter	NWS-MLB WSR-88D (Salazar et al. 2009)	45 SW Radtec 43/250 (Short 2008)
Wavelength	10.5 cm	5.32 cm
Frequency	S-band, 2.7 – 3.0 GHz	C-band, 5.6 – 5.65 GHz
Peak Power	750 kW	250 kW
Antenna diameter	8.5 m	4.3 m
Beam width	0.95°	0.95°
Rotation Rate	6 rpm	6 rpm
PRF	318 – 1304 s^{-1}	200 – 2000 s^{-1}
Pulse Length	1.57 and 4.7 μs	0.4 to 16.7 μs
Gain	45.5 dB	44 dB
Latitude	28.1131 N	28.3938 N
Longitude	80.6541 W	80.9510 W

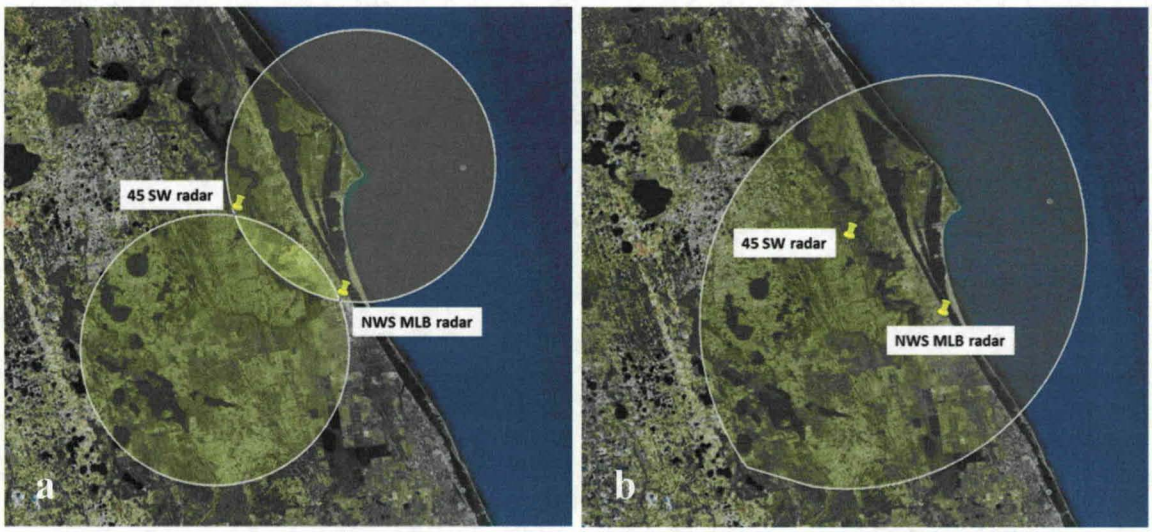

Figure 6. Same as Figure 4 except for the 45 SW and NWS MLB radars, where a) is area A_1 and b) is area A_2. The yellow pins show the locations of the radars. The white circles in a) are the dual-Doppler lobes within which the angles subtended by the radials from the radars lie between 30° and 150°. The intersecting area between the two circles along the radar baseline is not part of the dual-Doppler area because the beam crossing angles in this area are < 30° or > 150°. The white outline in b) shows area A_2, the outline of points that lie within a distance of 46.1 NM (85.3 km) of each radar.

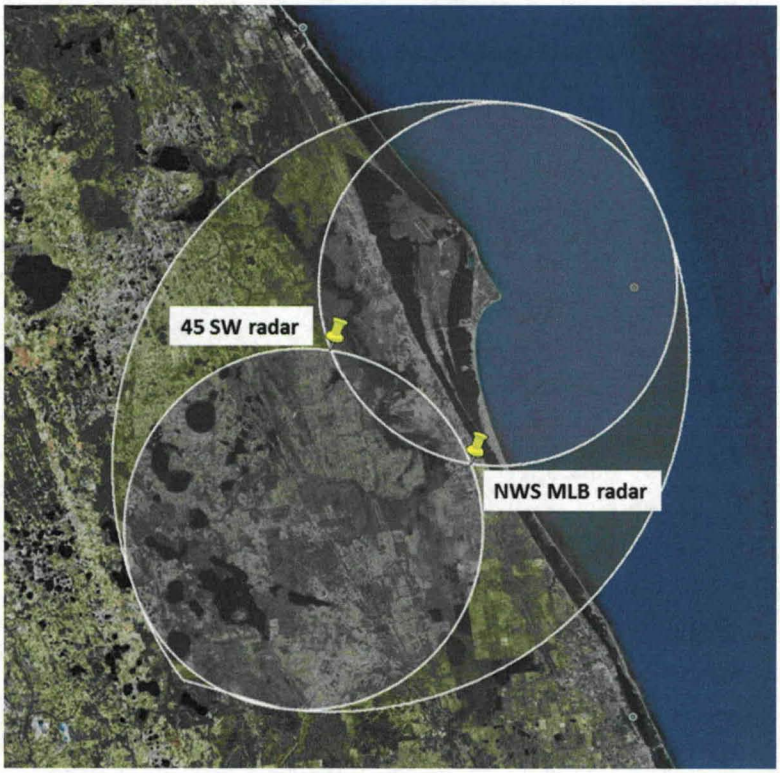

Figure 7. The intersection of areas A_1 and A_2 for the 45 SW and NWS MLB radars. The yellow pins show the locations of the radars.

Hardware and Software

There are several options to collect, edit, synthesize and display dual-Doppler data sets. The 45 SW currently uses the Interactive Radar Information System (IRIS™) software package by Vaisala to display their radar data. The IRIS™ software has an add-on product, called NDOP, that provides capability for Dual-Doppler wind fields based on radial wind inputs from two Doppler radars that can ingest WSR-88D data. Ingesting WSR-88D data also provides the opportunity to eliminate the cone of silence, an important issue for thunderstorms approaching from the southwest (a frequent trajectory in the summer). The license includes the ability to make mosaics, or composites, of radar products from multiple sites. The list cost is $16,000. This is a one-time cost for an add-on license to the existing IRIS software used by the 45 SW. An example of an IRIS™ NDOP product display is shown in Figure 8. Also a variety of freeware packages are available from the National Center for Atmospheric Research (NCAR) for processing raw radar data, but these packages do not have the thorough documentation and stringent configuration control needed in order to be certified for 45 SW use.

Regardless of software choice, a T1 data line must be installed between the Morrell Operations Center (MOC) on CCAFS and NWS MLB to enable the receipt of NWS MLB raw radar data needed for the dual-Doppler synthesis. This line, with additional costs, could also be used to send the 45 SW radar data to NWS MLB. In this case, NWS MLB can use the multi-sensor, multi-radar processing options via the Warning Decision Support System Integrated Information (WDSS-II) system for viewing the dual-Doppler radar data and then pass this information back to the 45 SW. The AMU could then create a way to view the dual-Doppler data using Meteorological Interactive Data Display System (MIDDS), Advanced Weather Interactive Processing System (AWIPS), or other display techniques. Due to the proprietary nature of the vendor costs of installing and maintaining the T1 line, performing drawing and configuration changes, and assuring information security functions, only a lower bound on the cost could be obtained from the 45 SW. The cost and time estimate given was a minimum of $150,000 and 6 to 12 months for this project. A monthly maintenance cost of the T1 line was estimated to be $1000.

Figure 8. An example of an NDOP Display for strong northerly winter monsoon flow over China near Hong Kong, colliding with easterlies over the sea. The "+" points show regions where the minimum crossing angle between radars was met, but there were no weather targets, so a wind could not be calculated. The green and gray contours indicate ~300 m (~1000 ft) elevation intervals (Vaisala IRIS™ Product and Display Manual 2006).

3. Summary and Conclusions

This study investigated technical, hardware, and software requirements necessary to enable the establishment of a dual-Doppler capability using the 45 SW Doppler and the NWS MLB WSR-88D radars. Use of these two Doppler radars to provide a 3-D display of the wind field will help forecasters to better predict the onset of convection and severe weather in support of space launch operations at KSC and CCAFS. The data can also be used to initialize a local mesoscale numerical weather prediction model to improve forecast output.

3.1 Dual-Doppler Analysis Feasibility

Evaluation of the physical locations and resulting beam crossing angles of the 45 SW and NWS MLB radars make them ideally suited for a dual-Doppler capability. The AMU derived the dual-Doppler equations to facilitate complete understanding of dual-Doppler synthesis, to determine the technical information requirements, and to determine how to find the three components of wind velocity from the equation of continuity and radial velocity data collected by two Doppler weather radars.

There are several options to collect, edit, synthesize and display dual-Doppler data sets. In addition to the commercially available Vaisala NDOP package available for purchase, there are a variety of freeware packages available including WDSS-II software available via license from the University of Oklahoma and from NCAR for processing raw radar data. Unfortunately, the freeware packages do not have sufficient documentation and configuration control to be certified for 45 SW use. In any case, a T1 data line must be installed between the MOC and NWS MLB to enable the receipt of NWS MLB raw radar data to use in the dual-Doppler synthesis. The installation of a T1 data line that will meet the security requirements necessary for 45 SW use is time-consuming and costly.

3.2 45 WS Interests

Possible applications for utilization of dual-Doppler data by the 45 WS are as follows. Note that due to the distance of the NWS MLB radar from sites on KSC/CCAFS, the beam altitude of the lowest beam may be too high to see some of the low level features suggested below:

- Easier visualization of wind fields for launch operation, pre-launch operations, wind warnings and wind forecasting.
- Easier detection of threatening convective winds.
- Better detection of convergence lines for forecasting convection initiation.
- Detection of low level helicity for severe weather prediction.
- Detection of winds near offshore for possible improved wind warnings.
- Initiation of short forecast local numerical models, especially the wind field over the ocean that is currently not measured well.
- Replacement of lost inland wind tower data to support 21st Century Spaceport or Air Force Smart Operations 21st Century (AFSO-21) initiative.

3.3 NWS MLB Interests

NWS MLB agrees that the siting of the two radars is ideal for use of dual-Doppler techniques at KSC and CCAFS. Once the 45 SW and NWS MLB radar data co-exist, NWS MLB can use the multi-sensor, multi-radar processing options via the Warning Decision Support System Integrated Information (WDSS-II) system for viewing. The WDSS-II is the second generation of a system of tools for the analysis, diagnosis and visualization of remotely sensed weather data. WDSS-II has the capability to merge multiple-radar data into four-dimensional grids including Terminal Doppler Weather Radar (TDWR) data. It is possible that both 45 SW radar data and TDWR data from Orlando International Airport could be used to alleviate radar geometry issues at the NWS MLB radar, such as the cone of silence or beam blockage. In addition, in the event of a radar outage at one of the sites, the multi-radar

algorithms would provide continuing coverage of the area through use of the data from the remaining operational radar sites.

3.4 Future Work

Accurate near-term forecasting of convective activity and severe storms is of continuing interest to all customers. As has been described, dual-Doppler capability can provide significant improvement to that forecasting capability. To illustrate the level of improvement that may be achieved, the AMU suggests the dual-Doppler data be subjected to a proof-of-concept activity by which wind data is validated to provide baseline confidence. Specifically, dual-Doppler data can be compared to balloon and/or wind profile data to evaluate and quantify the observed accuracy. These proof-of -concept evaluations could be performed on a variety of "typical" days including a summer day and a winter day when no convection or frontal zones are present and the normal sea breeze location is known. Once the data is validated and the capability has been confirmed, merged scans from the existing radars during known periods of convective activity and storms, such as that observed Oct 9 -10, 2011 (Columbus Day Storm) can be analyzed to determine if the dual-Doppler capability would have aided in the near-term forecasting.

Appendix

Derivation of the Dual-Doppler Equations

The following derivations were compiled from Armijo (1969), Obrien (1970), Lhermitte and Miller (1970) and Carey (2005). Before the Doppler radar data can be used to perform dual-Doppler wind retrieval, they must be converted from polar to Cartesian coordinates as follows (Goh and Holt 2004).

Referencing Figure 2, the distance between the target and radar 1 is:

$$R_1 = \sqrt{(x - x_1)^2 + (y - y_1)^2 + (z - z_1)^2} \tag{A-1}$$

The distance between the target and radar 2 is:

$$R_2 = \sqrt{(x - x_2)^2 + (y - y_2)^2 + (z - z_2)^2} \tag{A-2}$$

Squaring equations A-1 and A-2 above and taking the derivative of the squared radial velocities with respect to time will allow the distances to be converted to velocities that can then be solved to find the horizontal wind components:

$$R_1^2 = (x - x_1)^2 + (y - y_1)^2 + (z - z_1)^2 \tag{A-3}$$

$$R_2^2 = (x - x_2)^2 + (y - y_2)^2 + (z - z_2)^2 \tag{A-4}$$

$$2R_1 \frac{dR_1}{dt} = 2(x - x_1)\frac{dx}{dt} + 2(y - y_1)\frac{dy}{dt} + 2(z - z_1)\frac{dz}{dt} \tag{A-5}$$

$$2R_2 \frac{dR_2}{dt} = 2(x - x_2)\frac{dx}{dt} + 2(y - y_2)\frac{dy}{dt} + 2(z - z_2)\frac{dz}{dt} \tag{A-6}$$

Divide equation A-5 by $2R_1$ and substitute V_1 for $\frac{dR_1}{dt}$, u for $\frac{dx}{dt}$, v for $\frac{dy}{dt}$, and $w + V_t$ for $\frac{dz}{dt}$ to get:

$$V_1 = u\frac{(x - x_1)}{R_1} + v\frac{(y - y_1)}{R_1} + (w + V_t)\frac{(z - z_1)}{R_1} \tag{A-7}$$

Divide equation A-6 by $2R_2$ and substitute V_2 for $\frac{dR_2}{dt}$, u for $\frac{dx}{dt}$, v for $\frac{dy}{dt}$, and $w + V_t$ for $\frac{dz}{dt}$ to get:

$$V_2 = u\frac{(x - x_2)}{R_2} + v\frac{(y - y_2)}{R_2} + (w + V_t)\frac{(z - z_2)}{R_2} \tag{A-8}$$

Referencing **Error! Reference source not found.**, write equations A-7 and A-8 in terms of the radars' elevation (α) and azimuth (β) angles using the radar geometry as follows (Note: m denotes a generic radar number).

$$\frac{(x - x_m)}{R_m} = \cos\alpha_m \sin\phi_m, \quad \frac{(y - y_m)}{R_m} = \cos\alpha_m \cos\phi_m, \text{ and } \frac{(z - z_m)}{R_m} = \sin\alpha_m.$$

Using the above substitutions, equation A-7 becomes:

$$V_1 = u\cos\alpha_1 \sin\phi_1 + v\cos\alpha_1 \cos\phi_1 + (w + V_t)\sin\alpha_1. \tag{A-9}$$

Equation A-8 becomes:

$$V_2 = u\cos\alpha_2 \sin\phi_2 + v\cos\alpha_2 \cos\phi_2 + (w + V_t)\sin\alpha_2. \tag{A-10}$$

Solve equation A-9 for v:

$$v = \sec\alpha_1 \sec\phi_1 \left(-u\cos\alpha_1 \sin\phi_1 - (w + V_t)\sin\alpha_1 + V_1\right). \tag{A-11}$$

Substitute equation A-11 into equation A-10:

$$\begin{aligned} V_2 = {} & u\cos\alpha_2 \sin\phi_2 + \left(\sec\alpha_1 \sec\phi_1 \left(-u\cos\alpha_1 \sin\phi_1 - (w + V_t)\sin\alpha_1 + V_1\right)\right) \\ & * \cos\alpha_2 \cos\phi_2 + (w + V_t)\sin\alpha_2. \end{aligned} \tag{A-12}$$

Expand equation A-12 and multiply both sides of equation A-12 by cos β_1:

$$\begin{aligned} V_2 \cos\phi_1 = {} & u\cos\alpha_2 \sin\phi_2 \cos\phi_1 - u\cos\alpha_1 \sin\phi_1 \sec\alpha_1 \sec\phi_1 \cos\alpha_2 \cos\phi_2 \cos\phi_1 \\ & - (\mathrm{w} + \mathrm{V_t})\sin\alpha_1 \sec\alpha_1 \sec\phi_1 \cos\alpha_2 \cos\phi_2 \cos\phi_1 + V_1 \sec\alpha_1 \sec\phi_1 \cos\alpha_2 \cos\phi_2 \cos\phi_1 \\ & + (\mathrm{w} + \mathrm{V_t})\sin\alpha_2 \cos\phi_1. \end{aligned} \tag{A-13}$$

Simplify equation A-13:

$$\begin{aligned} V_2 \cos\phi_1 = {} & u\cos\alpha_2 \sin\phi_2 \cos\phi_1 - u\sin\phi_1 \cos\phi_2 \cos\alpha_2 \\ & - (\mathrm{w} + \mathrm{V_t})\tan\alpha_1 \cos\alpha_2 \cos\phi_2 + V_1 \sec\alpha_1 \cos\alpha_2 \cos\phi_2 \\ & + (\mathrm{w} + \mathrm{V_t})\sin\alpha_2 \cos\phi_1 \end{aligned} \tag{A-14}$$

Solve equation A-14 for u:

$$\begin{aligned} u\cos\alpha_2 (\sin\phi_1 \cos\phi_2 - \sin\phi_2 \cos\phi) = {} & V_1 \sec\alpha_1 \cos\alpha_2 \cos\phi_2 \\ & - V_2 \cos\phi_1 - (\mathrm{w} + \mathrm{V_t})\tan\alpha_1 \cos\alpha_2 \cos\phi_2 + (\mathrm{w} + \mathrm{V_t})\sin\alpha_2 \cos\phi_1 \end{aligned} \tag{A-15}$$

$$\begin{aligned} u = {} & \frac{V_1 \sec\alpha_1 \cos\alpha_2 \cos\phi_2}{\cos\alpha_2 (\sin\phi_1 \cos\phi_2 - \sin\phi_2 \cos\phi_1)} - \frac{V_2 \cos\phi_1}{\cos\alpha_2 (\sin\phi_1 \cos\phi_2 - \sin\phi_2 \cos\phi_1)} \\ & - \frac{(\mathrm{w} + \mathrm{V_t})\tan\alpha_1 \cos\alpha_2 \cos\phi_2}{\cos\alpha_2 (\sin\phi_1 \cos\phi_2 - \sin\phi_2 \cos\phi_1)} + \frac{(\mathrm{w} + \mathrm{V_t})\sin\alpha_2 \cos\phi_1}{\cos\alpha_2 (\sin\phi_1 \cos\phi_2 - \sin\phi_2 \cos\phi_1)} \end{aligned} \tag{A-16}$$

$$\begin{aligned} u = {} & \frac{1}{(\sin\phi_1 \cos\phi_2 - \sin\phi_2 \cos\phi_1)} \left[\frac{V_1 \cos\phi_2}{\cos\alpha_1} - \frac{V_2 \cos\phi_1}{\cos\alpha_2}\right] \\ & - (\mathrm{w} + \mathrm{V_t}) \left[\frac{\cos\phi_2 \tan\alpha_1 - \cos\phi_1 \tan\alpha_2}{(\sin\phi_1 \cos\phi_2 - \sin\phi_2 \cos\phi_1)}\right]. \end{aligned} \tag{A-17}$$

Substitute the trigonometric identity sin(u - v) = sin u cos v – cos u sin v in the denominator of equation A-17 (Lhermitte and Miller 1970):

$$u = \frac{1}{\sin(\phi_1 - \phi_2)} \left[\frac{V_1 \cos\phi_2}{\cos\alpha_1} - \frac{V_2 \cos\phi_1}{\cos\alpha_2}\right] - (\mathrm{w} + \mathrm{V_t}) \left[\frac{\cos\phi_2 \tan\alpha_1 - \cos\phi_1 \tan\alpha_2}{\sin(\phi_1 - \phi_2)}\right]. \tag{A-18}$$

Solve for v by repeating the above steps. Solve equation A-10 for u:

$$u = \sec\alpha_2 \csc\phi_2 \left(-v\cos\alpha_2 \cos\phi_2 - (w + V_t)\sin\alpha_2 + V_2\right). \tag{A-19}$$

Substitute equation A-19 into equation A-9:

$$V_1 = [\sec\alpha_2 \csc\phi_2(-v\cos\alpha_2\cos\phi_2 - (w+V_t)\sin\alpha_2 + V_2)]\cos\alpha_1\sin\phi_1 + v\cos\alpha_1\cos\phi_1 + (w+V_t)\sin\alpha_1. \quad \text{(A-20)}$$

Expand equation A-20 and multiply both sides of equation A-12 by sin β_2:

$$V_1\sin\phi_2 = -v\cos\alpha_2\cos\phi_2\cos\alpha_1\sin\phi_1\sec\alpha_2\csc\phi_2\sin\phi_2 + v\cos\alpha_1\cos\phi_1\sin\phi_2 - (w + V_t)\sin\alpha_2\sec\alpha_2\csc\phi_2\cos\alpha_1\sin\phi_1\sin\phi_2 + V_2\sec\alpha_2\csc\phi_2\cos\alpha_1\sin\phi_1\sin\phi_2 + (w + V_t)\sin\alpha_1\sin\phi_2. \quad \text{(A-21)}$$

Simplify equation A-21:

$$V_1\sin\phi_2 = -v\cos\phi_2\cos\alpha_1\sin\phi_1 + v\cos\alpha_1\cos\phi_1\sin\phi_2 - (w + V_t)\tan\alpha_2\cos\alpha_1\sin\phi_1 + V_2\sec\alpha_2\cos\alpha_1\sin\phi_1 + (w + V_t)\sin\alpha_1\sin\phi_2. \quad \text{(A-22)}$$

Solve equation A-22 for v:

$$v\cos\alpha_1(\cos\phi_2\sin\phi_1 - \sin\phi_2\cos\phi_1) = V_2\sec\alpha_2\cos\alpha_1\sin\phi_1 - V_1\sin\phi_2 - (w + V_t)\tan\alpha_2\cos\alpha_1\sin\phi_1 + (w + V_t)\sin\alpha_1\sin\phi_2 \quad \text{(A-23)}$$

$$v = \frac{V_2\sec\alpha_2\cos\alpha_1\sin\phi_1}{\cos\alpha_1(\sin\phi_1\cos\phi_2 - \sin\phi_2\cos\phi_1)} - \frac{V_1\sin\phi_2}{\cos\alpha_1(\sin\phi_1\cos\phi_2 - \sin\phi_2\cos\phi_1)} - \frac{(w + V_t)\tan\alpha_2\cos\alpha_1\sin\phi_1}{\cos\alpha_1(\sin\phi_1\cos\phi_2 - \sin\phi_2\cos\phi_1)} + \frac{(w + V_t)\sin\alpha_1\sin\beta_2}{\cos\alpha_1(\sin\phi_1\cos\phi_2 - \sin\phi_2\cos\phi_1)} \quad \text{(A-24)}$$

$$v = \frac{1}{(\sin\phi_1\cos\phi_2 - \sin\phi_2\cos\phi_1)}\left[\frac{V_2\sin\phi_1}{\cos\alpha_2} - \frac{V_1\sin\phi_2}{\cos\alpha_1}\right] - (w + V_t)\left[\frac{\sin\phi_1\tan\alpha_2 - \sin\phi_2\tan\alpha_1}{(\sin\phi_1\cos\phi_2 - \sin\phi_2\cos\phi_1)}\right]. \quad \text{(A-25)}$$

Substitute the trigonometric identity sin(u - v) = sin u cos v – cos u sin v in the denominator of equation A-25 (Lhermitte and Miller 1970):

$$v = \frac{1}{\sin(\phi_1 - \phi_2)}\left[\frac{V_2\sin\phi_1}{\cos\alpha_2} - \frac{V_1\sin\phi_2}{\cos\alpha_1}\right] - (w + V_t)\left[\frac{\sin\phi_1\tan\alpha_2 - \sin\phi_2\tan\alpha_1}{\sin(\phi_1 - \phi_2)}\right]. \quad \text{(A-26)}$$

Now there are two equations, A-18 and A-26, with four unknowns: u, v, w, and V_t. Therefore, equations A-18 and A-26 must be supplemented with the equation of continuity:

$$\frac{\partial\rho}{\partial t} + \frac{\partial(\rho u)}{\partial x} + \frac{\partial(\rho v)}{\partial y} + \frac{\partial(\rho w)}{\partial z} = 0. \quad \text{(A-27)}$$

Expand equation A-27 to get:

$$\frac{\partial\rho}{\partial t} + \rho\frac{\partial u}{\partial x} + u\frac{\partial\rho}{\partial x} + \rho\frac{\partial v}{\partial y} + v\frac{\partial\rho}{\partial y} + \rho\frac{\partial w}{\partial z} + w\frac{\partial\rho}{\partial z} = 0 \quad \text{(A-28)}$$

Assume density, ρ, is constant at a particular level, z, and simplify equation A-28:

$$\rho\frac{\partial u}{\partial x}+\rho\frac{\partial v}{\partial y}+\rho\frac{\partial w}{\partial z}+w\frac{\partial \rho}{\partial z}=0. \tag{A-29}$$

Rearrange equation A-29:

$$\rho\frac{\partial w}{\partial z}+w\frac{\partial \rho}{\partial z}=-\left(\rho\frac{\partial u}{\partial x}+\rho\frac{\partial v}{\partial y}\right). \tag{A-30}$$

Substitute $\frac{\partial(\rho w)}{\partial z}=\rho\frac{\partial w}{\partial z}+w\frac{\partial \rho}{\partial z}$ into equation A-30:

$$\frac{\partial(\rho w)}{\partial z}=-\left(\rho\frac{\partial u}{\partial x}+\rho\frac{\partial v}{\partial y}\right). \tag{A-31}$$

Now, equation A-31 can be integrated from one level to the next for each level:

$$\int_a^b\frac{\partial(\rho w)}{\partial z}=-\int_a^b\left(\rho\frac{\partial u}{\partial x}+\rho\frac{\partial v}{\partial y}\right) \tag{A-32}$$

$$(\rho w)_b-(\rho w)_a=-\left[\rho\left(\frac{\partial u}{\partial x}+\frac{\partial v}{\partial y}\right)_b\Delta z-\rho\left(\frac{\partial u}{\partial x}+\frac{\partial v}{\partial y}\right)_a\Delta z\right]. \tag{A-33}$$

Equation A-33 can be solved for vertical velocity, w, at every height by first assuming w=0 at the surface and then iterating until the mean difference between the horizontal and vertical divergence is less than some predetermined threshold.

Finally, V_t can be estimated by using standard V_t-Z relationships (Doviak et al. 1976):

$$V_t=2.65Z^{0.114}\left(\frac{\gamma_0}{\gamma}\right)^{0.4}\left[ms^{-1}\right]. \tag{A-34}$$

The IRIS NDOP software estimates V_t using the following relationships (IRIS 2006):

Above the melting level (snow and graupel): $V_t=0.8Z^{0.06}\left[ms^{-1}\right]$ (A-35)

Below the melting level (rain): $V_t=2.70Z^{0.11}\left[ms^{-1}\right]$ (A-36)

List of Acronyms

45 SW	45th Space Wing
45 WS	45th Weather Squadron
AMU	Applied Meteorology Unit
AWIPS	Advanced Weather Interactive Processing System
CCAFS	Cape Canaveral Air Force Station
IRIS™	Interactive Radar Information System
KSC	Kennedy Space Center
MIDDS	Meteorological Interactive Data Display System
MLB	Melbourne, Fla. – 3 letter identifier
MOC	Morrell Operations Center
NASA	National Aeronautics and Space Administration
NCAR	National Center for Atmospheric Research
NDOP	IRIS product that calculates dual-Doppler wind fields based on radial wind inputs from two Doppler radars
NM	Nautical Mile
NSSL	National Severe Storms Laboratory
NWS	National Weather Service
TDWR	Terminal Doppler Weather Radar
WDSS-II	Warning Decision Support System Integrated Information
WSR-88D	Weather Surveillance Radar - 1988 Doppler

References

Armijo, L., 1969: A Theory for the Determination of Wind and Precipitation Velocities with Doppler Radars, *J. Atmos. Sci.*, **26**, 570-575.

Beck, J., 2004: High-Resolution Dual-Doppler Analyses of the 29 May 2001 Kress, TX, Cyclic Supercell. Masters Thesis, Texas Tech University, 109 pp.

Bousquet, O., P. Tabary, and J. Parent du Châtelet, 2008: Operational Multiple-Doppler Wind Retrieval Inferred from Long-Range Radial Velocity Measurements, *J. Appl. Meteor.*, **47**, 2929-2945.

Carey, L., 2005: Houston Advanced Research Center, Texas Environmental Research Consortium. Final Progress Report for the Deployment of the C-band Radars to DFW and HGB for the 2005 Ozone Season, 47 pp.

Davies-Jones, R., 1979: Dual-Doppler Radar Coverage Area as a Function of Measurement Accuracy and Spatial Resolution, *J. Appl. Meteor.*, **18**, 1229-1233.

Doviak, R. and D. Zrnic, 1993: *Doppler Radar and Weather Observations*, 2nd Ed., Academic Press, San Diego, CA, 562 pp.

Doviak, R., P. Ray, R. Strauch and L. Miller, 1976: Error Estimation in Wind Fields Derived from Dual-Doppler Radar Measurement, *J. Appl. Meteor.*, **15**, 868-878.

Friedrich, K. and M. Hagen, 2004: On the Use of Advanced Doppler Radar Techniques to Determine Horizontal Wind Fields for Operational Weather Surveillance, *Meteorol. Appl.*, **11**, 155-171.

Goh, Y. and A. Holt, 2004: Analysis of Three-dimensional Wind Fields from Two Operational Doppler Radars, *Proceedings of ERAD 2004 (European Conference on Radar in Meteorology and Hydrology)*, Visby, Sweden, Sept. 6-10, 2004, 35-40.

IRIS Product and Display Manual, Configuring IRIS Products NDOP, Vaisala Corp., January 2006, pp. 3-46 to 3-54.

Lakshmanan, V., T. Smith, G. Stumpf, and K. Hondl, 2007: The Warning Decision Support System-Integrated Information, *Wea. Forecasting*, **22**, 596-612.

Lhermitte, R. and L. Miller, 1970: Doppler Radar Methodology for the Observation of Convective Storms. *14th Conf. on Radar Meteor.*, Tuscon, AZ, Amer. Meteor. Soc., 133-138.

Obrien, J., 1970: Alternative Solutions to the Classical Vertical Velocity Problem, *J. Appl. Meteor.*, **9**, 197-203.

Rinehart, R., 2004: *Radar for Meteorologists*, 4th Ed., Rinehart Publications, Columbia, MO, 482 pp.

Salazar, J., A. Hopf, R. Contreras, B. Philips, E. Knapp, D. McLaughlin, J. Brotzge, and K. Brewster, 2009: Coverage Comparison of Short Range Radar Networks vs. Conventional Weather Radars: Case Study in the Northwestern United States. *Proc. Geoscience and Remote Sensing Symp., IGARSS'09,* Vol. 2, Cape Town, South Africa, IEEE, 964-967.

Short, D., 2008: Radar Scan Strategies for the Patrick Air Force Base Weather Surveillance Radar, Model 74C, Replacement. NASA Contractor Report CR-2008-214745, Kennedy Space Center, FL, 28 pp. [Available from ENSCO, Inc., 1980 N. Atlantic Ave., Suite 830, Cocoa Beach, FL, 32931 and online at http://science.ksc.nasa.gov/amu/final.html.]

NOTICE

Mention of a copyrighted, trademarked or proprietary product, service, or document does not constitute endorsement thereof by the author, the AMU, the National Aeronautics and Space Administration, or the United States Government. Any such mention is solely for the purpose of fully informing the reader of the resources used to conduct the work reported herein.